PL-TR--93-1092

E202012

PL-TR--93-1092

RADIAL ACCELETRON, A NEW LOW IMPEDANCE HPM SOURCE

AD-A282 008

M. Joseph Arman
Kyle J. Hendricks

March 1994

Final Report

APPROVED FOR PUBLIC RELEASE; DISTRIBUTION IS UNLIMITED.

94-18220

21P8

PHILLIPS LABORATORY
Advanced Weapons and Survivability Directorate
AIR FORCE MATERIEL COMMAND
KIRTLAND AIR FORCE BASE, NM 87117-5776

94 6 13 112

This final report was prepared by the Phillips Laboratory, Kirtland Air Force Base, New Mexico, under Job Order 5797AK04. Dr. Kirk Hackett (WSR) was the Phillips Laboratory Project Officer-in-Charge.

This technical report has been reviewed and is approved for publication.

Moossa Arman

MOOSSA JOSEPH ARMAN, Ph.D.
Research Physicist, Electromagnetic
Sources Division

FOR THE COMMANDER

FORREST J. AGEE
Chief, Electomagnetic Sources
Division

BRENDAN B. GODFREY
Acting Director, Advanced Weapons
and Survivability Directorate

REPORT DOCUMENTATION PAGE	Form Approved OMB No. 0704-0188

1. AGENCY USE ONLY (Leave blank)	2. REPORT DATE	3. REPORT TYPE AND DATES COVERED
	March 1994	Final Nov 91 - Oct 92

4. TITLE AND SUBTITLE

RADIAL ACCELETRON, A NEW LOW IMPEDANCE HPM SOURCE

5. FUNDING NUMBERS

PE: 62601F
PR: 5797
TA: AK
WU: 04

6. AUTHOR(S)

M. Joseph Arman, Kyle J. Hendricks

7. PERFORMING ORGANIZATION NAME(S) AND ADDRESS(ES)

Phillips Laboratory
3550 Aberdeen SE
Albuquerque, NM 87117-5776

8. PERFORMING ORGANIZATION REPORT NUMBER

PL-TR--93-1092

9. SPONSORING/MONITORING AGENCY NAME(S) AND ADDRESS(ES)

10. SPONSORING/MONITORING AGENCY REPORT NUMBER

11. SUPPLEMENTARY NOTES

This research was funded IN PART by the National Academy of Sciences, National Research Council.

12a. DISTRIBUTION/AVAILABILITY STATEMENT

Approved for public release; Distribution is unlimited.

12b. DISTRIBUTION CODE

13. ABSTRACT *(Maximum 200 words)*

This report explores and analyzes using transit-time effects in a coaxial geometry to develop a low-impedance high power microwave (HPM) source that uses no external magnetic field and no confining foils. This source works in the 1-20 GHz range and has a power output of no less than 1 GW. The input is a low-voltage dc pulse of only 350 kV or less with a flat top of ~200 ns. The dc pulse is launched into a coaxial structure comprised of the diode, the oscillator, and the buncher. Strong impedance mismatch between the diode section and the body of the device provides enough reflection to have a well defined coaxial cavity of high Q to support cavity characteristic modes. Electrons emitted from the inner conductor of the structure accelerate toward the anode interacting with a selected characteristic mode of the structure, usually losing kinetic energy to the mode, until the RF fields are strong enough to optimize, thus leading to saturation. The source offers significant improvements in power, repetition rate, size, and efficiency because of the coaxial structure. The diode impedance may be reduced to a few ohms thus allowing larger input and output powers. With no foils to erode, the only thing limiting the repetition rate is the vacuum ability and, with no external magnetic field required, the device is simple, lightweight, and inexpensive. Because of the strong bunching, the efficiency is high and, as with all transit-time oscillators, the signal is stable and monochromatic. The device may be used as a buncher or as an oscillator.

14. SUBJECT TERMS

High Power Microwave, HPM, Low Impedance, High Repetition Rate, Radial Acceletron

15. NUMBER OF PAGES 17

16. PRICE CODE

17. SECURITY CLASSIFICATION OF REPORT	18. SECURITY CLASSIFICATION OF THIS PAGE	19. SECURITY CLASSIFICATION OF ABSTRACT	20. LIMITATION OF ABSTRACT
Unclassified	Unclassified	Unclassified	SAR

NSN 7540-01-280-5500

Standard Form 298 (Rev. 2-89)
Prescribed by ANSI Std Z39-18
298-102

CONTENTS

FIGURES

1.0 INTRODUCTION

Accelerated motion of electric charges is the source of all electromagnetic radiations. Fields of characteristics modes of high Q conducting structures can be used as an accelerating mechanism for coherent radiation from charged particle beams in the microwave range (Refs. 1-5). For instance, when streaming charged particles cross a cavity resonating at one of its characteristic modes, decelerating fields of the mode, under certain conditions, can cause the charges to radiate coherently, thereby losing some of their kinetic energy and enhancing the fields. This process, known as the "Transit-Time" effect, has been understood since the 1930s. However, mainly because of very low growth rate and partly because of low saturation levels, no significant amount of microwave radiation has been produced with the nonrelativistic charged particle beams available until now. An attempt at increasing the beam current in order to increase the power could result in strong space charge depression and formation of a virtual cathode. Recent advances in pulse-power technology has made relativistic giga-amp beams possible thereby reviving the Transit-Time Oscillators (TTO) as a possible source of High Power Microwave (HPM) radiation. Since the resonating structure has a strong stabilizing effect on the process, HPM sources based on TTOs are robust, stable, monochromatic, and efficient.

The radial acceletron is one such new source. Its cylindrical structure allows a very low impedance (high power) and oscillator combined with the diode uses no foil so the repetition rate can be very high. Furthermore, for the modes explored here, the radial acceletron uses no external magnetic field so it is very compact and light. In Section 2.0 the theory involved in the radial acceletron is explored. The results of numerical simulations are presented in Section 3.0. Section 4.0 is the conclusion and suggestions for follow-up work.

2.0 THEORY

This is a brief qualitative description of the theory of TTOs. When charged particles cross a structure with standing RF waves they undergo a series of accelerations and decelerations. If the particles' transit-time is close to the period of the RF and the radiation is the lowest mode in the direction of the transit, there will be one acceleration and one deceleration in an order that depends on the phase at the time of entry. Those particles accelerating on entry and then decelerating will travel faster than the average and will gain some kinetic energy upon leaving. Those particles entering in a decelerating phase, however, will spend more time in the cavity than the average transit time. These particles will lose more kinetic energy than those of the opposite phase gained. The overall result is a net flow of energy from the beam to the fields. This process continues until the average transit time becomes significantly different from the initial transit time and the fields cease to grow any further.

In an acceletron this process takes place in a diode and the particles are, in addition to the RF fields, also subject to the dc fields of the diode. This not only allows for a more compact system because the diode and the resonating cavity are combined into one, the uniform acceleration due to the dc fields raises the space charge limited current, thus allowing more current at a lower voltage. Combining the diode and the resonator also eliminates the need for foils in the path of the beam thus allowing for very high repetition rate.

In a *radial* acceletron, in addition, the diode/resonator has a coaxial structure that allows for much smaller diode impedances and consequently higher power for any given voltage. Figure 1 is a schematic drawing of a radial acceletron with coaxial loading. It consists of two coaxial lines sharing the same outer conductor. The inner conductor to the left is the cathode, enlarged at the emission area to enhance the fields and to increase the emission surface. The dc pulse is launched from the left. The electrons move radially towards the anode and radiate in the process. The radiation is extracted through the coaxial line to the right.

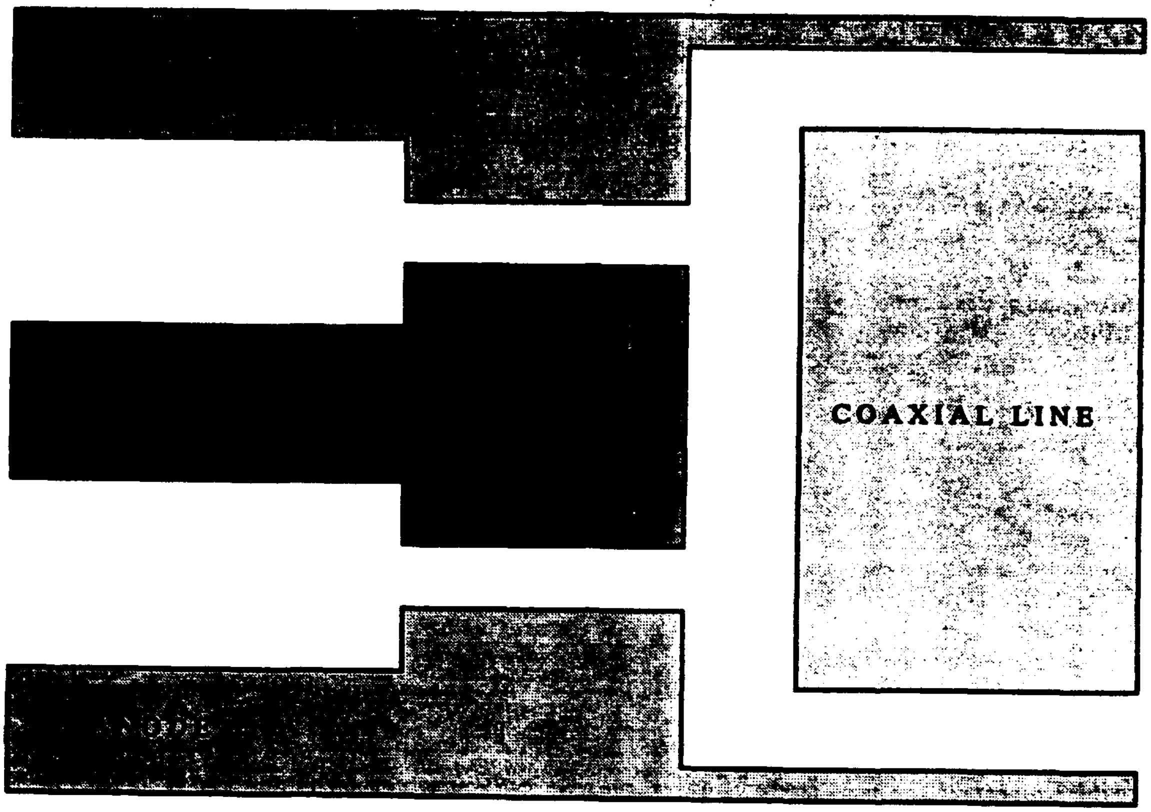

Figure 1. Schematic plot of the radial acceletron with radial loading.
The dc pulse is launched from the left.

The most complete solution to the radial acceletron problem is to solve the Maxwell's equations for the entire system and find the fields and the current self-consistently as a function of time. This approach is, however, intractable because of the complicated boundary conditions involved. In the small-signal gain approximation the fields are initially assumed to be known, eigen modes of the system, and the current is assumed to be fixed. The nonlinear effects, if any, and the space charge effect are ignored in this approximation, and the saturation mechanism cannot be addressed. In this approximation, the energy exchange between the beam and the RF radiation may be described by

$$\frac{d(Energy)}{dt} = \int_{beam} (\vec{J} \cdot \vec{E})dV \qquad (1)$$

where J is the beam current, E is the sum of the dc field and the electric field of the eigen mode assumed to be present in the cavity, and the integration is over the beam volume. Furthermore, to assure analytic solution, nonrelativistic approximation is used and the calculation is carried out for a single particle. Generalization to a stream is trivial.

Assuming a TM_{001} mode and a rectangular approximation to the eigen mode in the coaxial cavity, integrate the equation of motion to get

$$v = \frac{eV}{md}t + \frac{eE_0}{m\omega}(sin(\omega t + \phi) - sin\phi) \qquad (2)$$

where v is the velocity of the electron as a function of time, e is the electron charge, V is the dc voltage, m is the electron mass, d is the diode gap, E_0 is the amplitude of the assumed RF field, RF is the angular frequency of the RF, and ϕ is the phase at which the particle was emitted. Integrating Equation 2 with respect to t over the gap gives

$$d = \frac{eV}{2md}\tau^2 - \frac{eE_0 sin\phi}{m\omega}\tau - \frac{eE_0}{m\omega^2}(cos(\omega\tau + \phi) - cos\phi) \qquad (3)$$

where τ is the transit time of the electron. If it is further assumed that the transit time τ is comparable to the period T of the RF, Equation 3 reduces to

$$d = \frac{eV}{2md}\tau^2 - \frac{eE_0 sin\phi}{m\omega}\tau \qquad (4)$$

Solving for τ and assuming $E_0 << (V/d)$

$$\tau = \left(\frac{E_0 \sin\phi}{\omega V} - \sqrt{\frac{2m}{eV}}\right)d \tag{5}$$

Substituting Equation 5 in Equation 2 gives the final velocity v_f as a function of ϕ, V, and d

$$v_f = \left(\frac{eE_0 \sin\phi}{m\omega} - \sqrt{\frac{2eV}{m}}\right) + \frac{eE_0}{m\omega}\left[\sin\left(\frac{E_0 d \sin\phi}{V} - \omega d\sqrt{\frac{2m}{eV}} + \phi\right) - \sin\phi\right] \tag{6}$$

The velocity gain due to the RF, vd, is given by

$$v_d = v_{dc} - v_f = \sqrt{\frac{2eV}{m}} - v_f \tag{7}$$

where v_{dc} is the final velocity in the absence of RF. The v_d averaged over ϕ changes sign with d displaying alternating regions of growth and damping as a function of d. The v_d is a measure of how much energy is being exchanged between the beam and the RF. This quantity may be summed over all electrons to find the growth rate for the RF radiation.

3.0 SIMULATION

The TM_{001} mode of the radial acceletron has been studied rather extensively using the 2-D PIC codes ISIS and MAGIC and the 3-D PIC code SOS. The 2-D simulations were carried out to verify the principle behind the radial acceletron and to confirm its viability as an HPM source. The 3-D simulations were performed to rule out the presence of nonaxisymmetric modes that could disturb the TM_{001} mode. A tentative axial loading of the device was also modeled using the 2-D code MAGIC. An unoptimized rms efficiency of 15 percent has been observed.

3.1 THE 2-D SIMULATIONS

The 2-D simulations were carried out for a device designed to produce the TM_{001} mode at 3.1 GHz operating at 300 kv. The choice of the TM_{001} mode was arbitrary: other modes and other frequencies are equally achievable. The radius of the inner conductor at the emission surface, Figure 1, is 23.4 cm, the radius of the anode is 27.0 cm, and the cavity is 6.4 cm long. The emission surface is 3.2 cm long. The input line impedance is 20 Ω, the load impedance is 4 Ω and the gap between the diode and the load is 8 cm. A short rise time of 5 ns for the dc pulse was applied to speed up the simulation. In some simulations Bragg reflectors were used in the input line to increase the Q of the cavity.

Figure 2 is a plot of particle trajectories as they move towards the anode. This corresponds to a time when the instability has saturated and the emission is fully modulated by the RF's electric field. In addition to this modulation, interaction with the RF has further bunched the beam to very high densities, an indication of possible high efficiency. Figure 3 is a perspective plot of the radial electric field showing the RF propagating along the gap and down the coaxial load to the right. The Bragg reflectors in the input line have reduced the backward going RF to a very low level. Notice that the peak values of the RF amplitude in the coaxial load is larger than the dc amplitude in the input line.

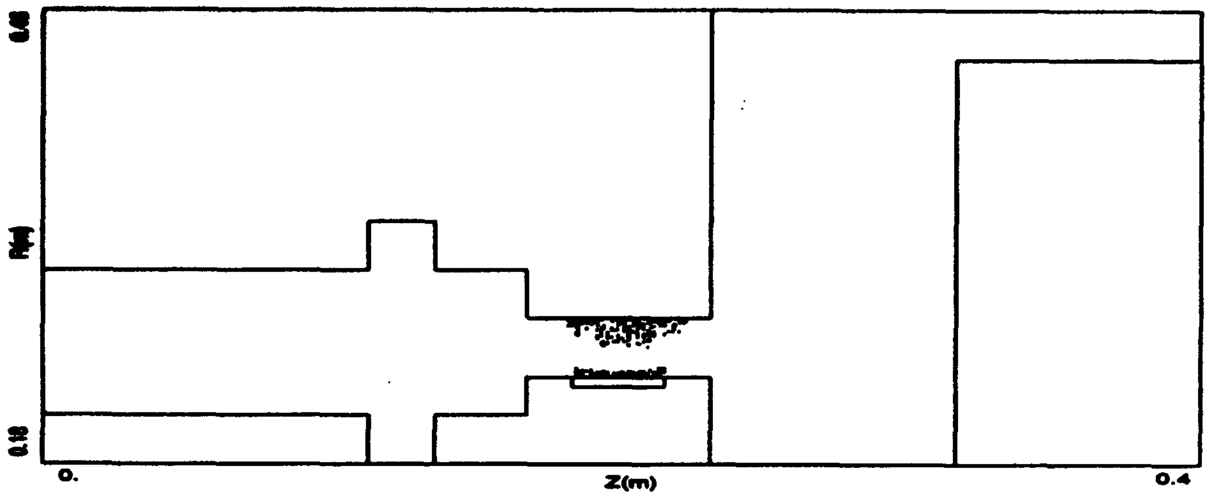

Figure 2. Computer simulation of the radial acceletron showing the electron in a gated emission pattern. The Bragg reflectors in the input line are for confining the RF fields. Only the upper portion of the device is modeled.

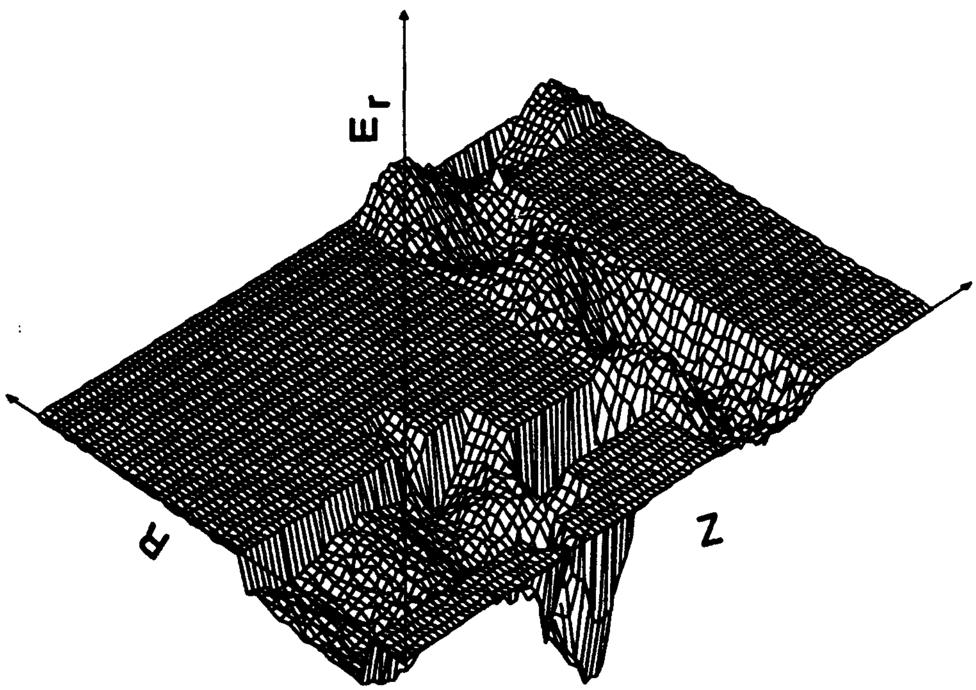

Figure 3. Perspective plot of the radial electric field showing the RF being generated in the cavity, propagating radially outward towards the coaxial line and leaving the system through the coax.

Figure 4a is the voltage in the center of the diode (i.e., E, at the center integrated along the radius) plotted as a function of time. The amplitude of the RF is slightly larger than the magnitude of the input pulse. Figure 4b is the Fourier transform of 4a. Tt shows a pure TM_{001} mode with no indication of any mode competition. Figure 5 is the time plot of the radial current density in amps per meter. The total dc current, $2\pi r j_r$, is ~10 ka. The peak RF current is ~4 times that, indicating very strong bunching. The Fourier analysis of the current time plot shows up to 6 harmonics present. The enlargement of the current plot shows regions of zero current caused by emission turn-off due to strong RF fields at the cathode. This modulated emission feature is similar to the gated emission patterns much desired in many RF related applications of intense electron beams.

Figure 6a is a plot of the extracted RF power as a function of time. The peak power is ~500 mw, leading to an rms efficiency of 15 percent. No effort so far has been made in optimizing the loading and the extraction mechanism. Based on the bunching properties of the beam, the author is confident an overall rms efficiency of 25 percent is readily possible. Figure 6b is the Fourier transform of 6a showing the main peak at twice the frequency of the RF radiation. This indicates the extracted power is almost entirely ac radiation.

The Appendix is a sample copy of a typical input file to the PIC code MAGIC used extensively in this work.

3.2 THE 3-D SIMULATIONS

The purpose of the 3-D simulations was to rule out the possibility of mode competition due to nonaxisymmetric modes. The acceletron with the TM_{001} mode is basically a 2-D problem. However, to model the nonaxisymmetric modes one needs to model the entire device. The device modeled in 2-D was also modeled in 3-D with the azimuthal angle ranging from 0 to 360 degrees, in cylindrical geometry. The gridding was chosen to resolve any modes at TM_{333} or lower. No mode other than the TM_{001} mode was observed for the parameters used. Figure 7 is a plot of the Fourier transform of the beam current from the 3-D simulation indicating there are no modes other than the mode observed in the 2-D simulation.

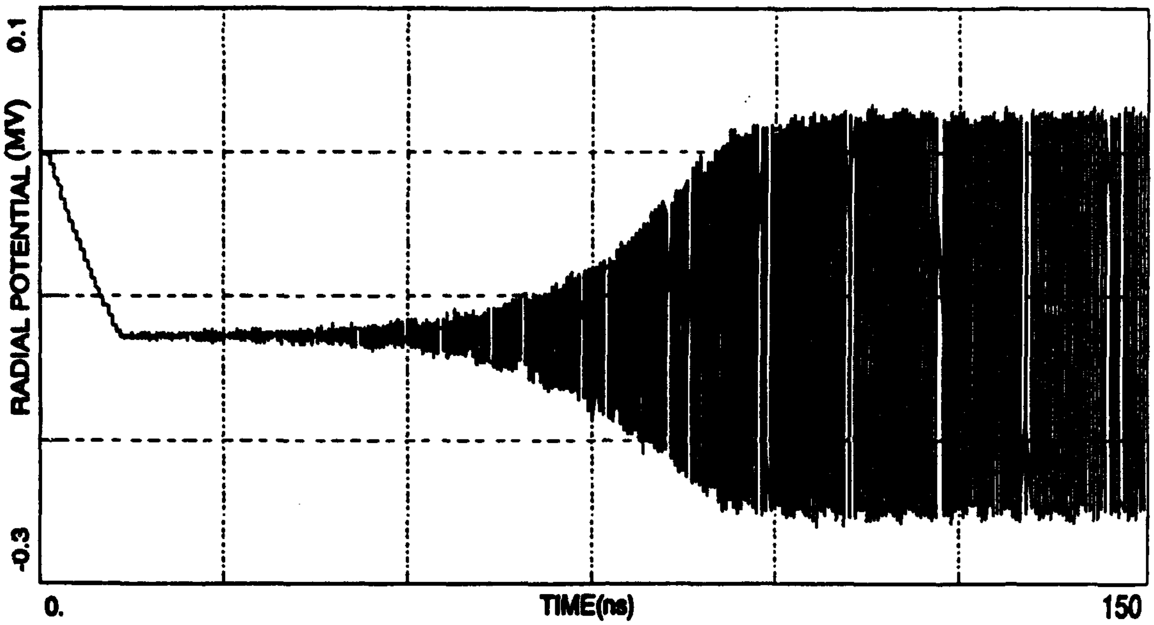

(a) Time plot of the radial potential at the center of the resonator cavity. The amplitude of the ac voltage exceeds the dc value by a small fraction.

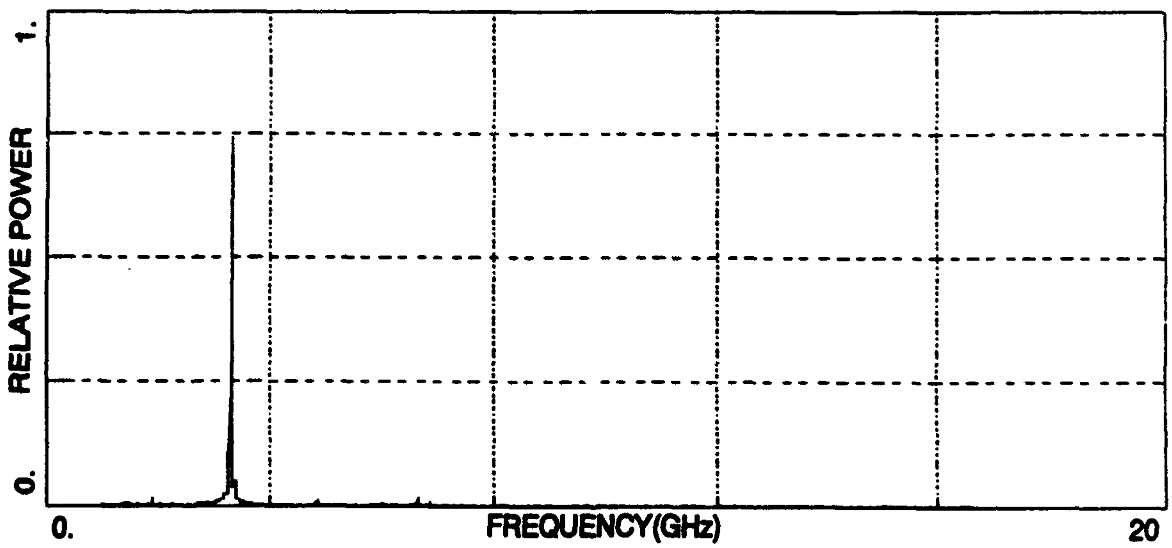

(b) The Fourier transform of 4a showing a stable signal at ~3.1 GHz.

Figure 4. Potential at the center of the resonator cavity.

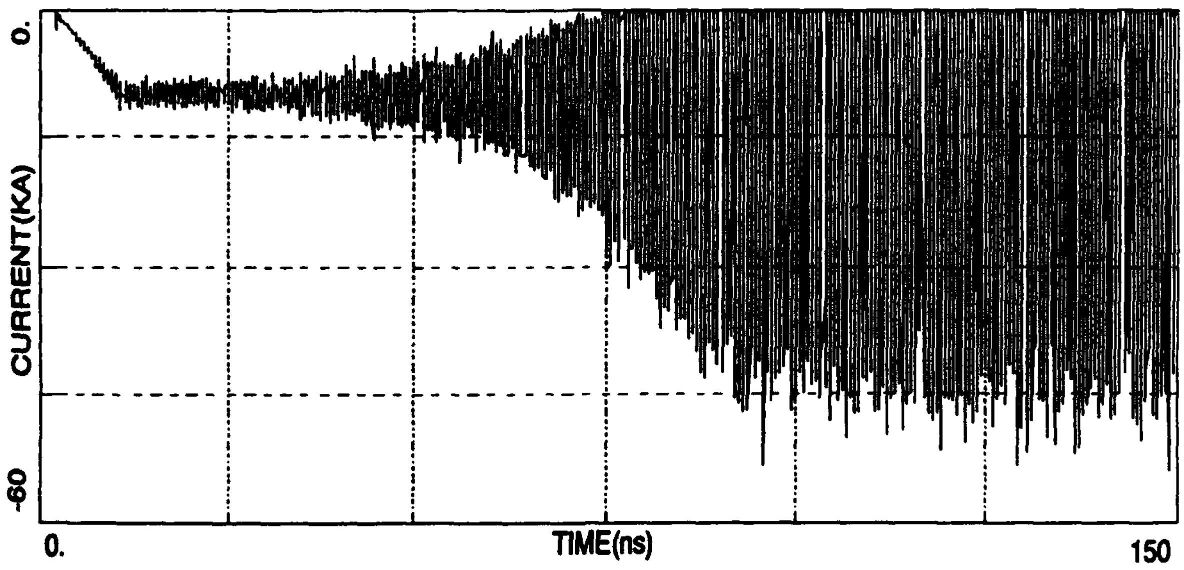

Figure 5. The time plot of the total radial current in the resonator cavity. The peak ac current is at least 4 times the dc level, an indication of a strongly bunched beam.

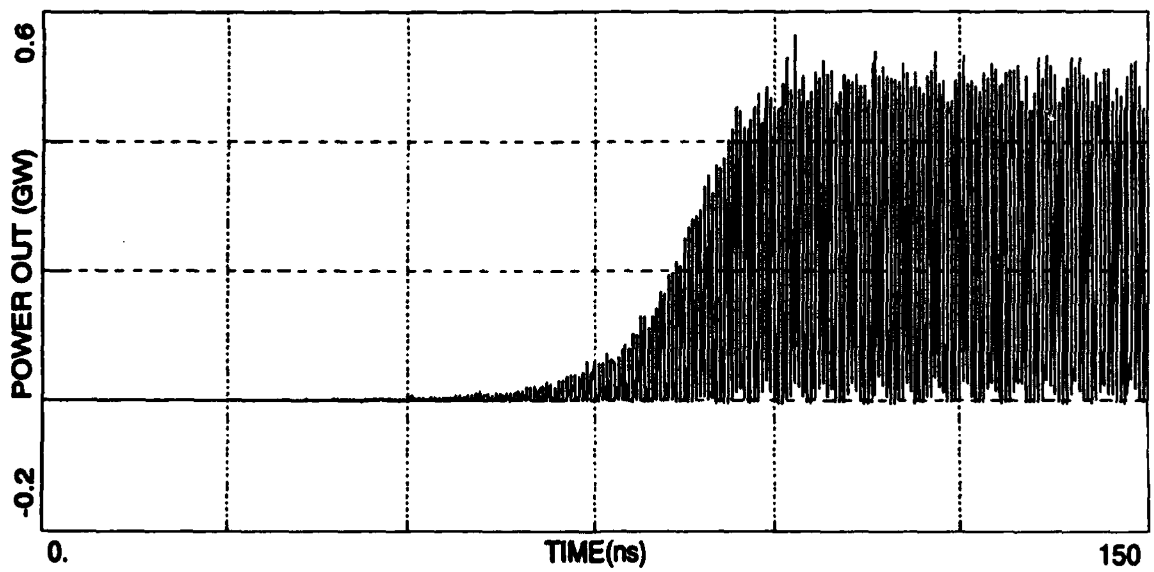

(a) The time plot of the extracted power through a coaxial load showing a stable RF signal. The axial load is not optimized and the choice of axial extraction is not final.

Figure 6. Extracted Power.

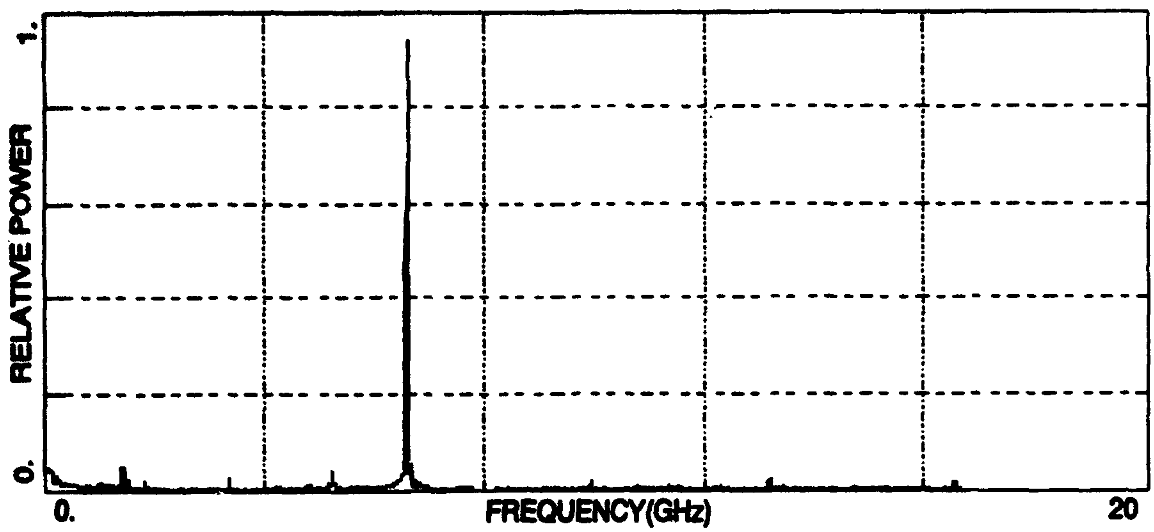

(b) The Fourier transform of 6a showing a monochromatic RF signal at twice the frequency of the RF fields.

Figure 6. (Concluded).

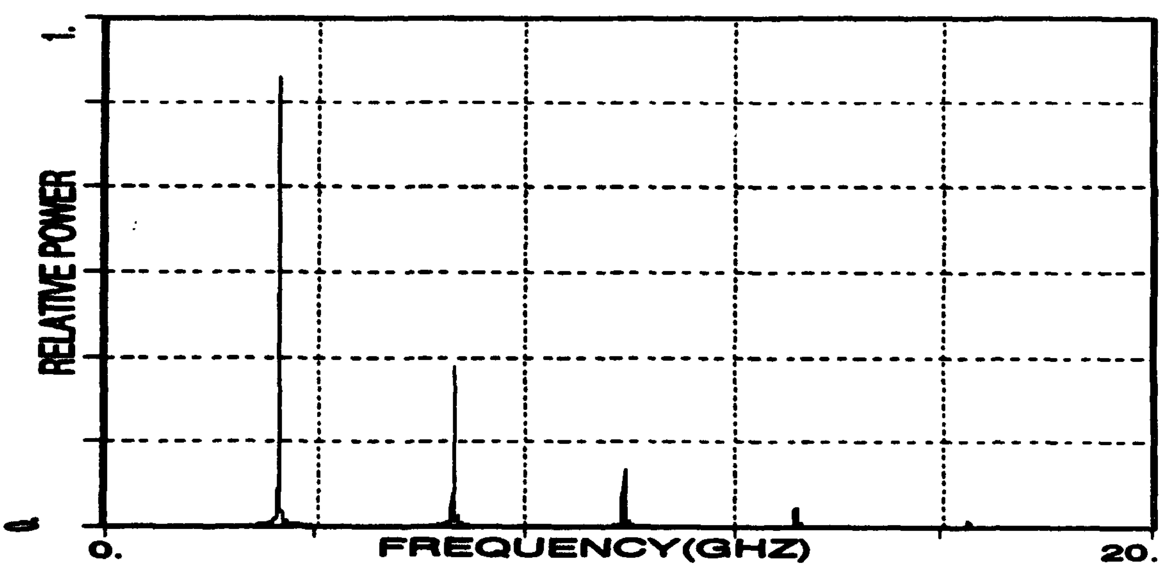

Figure 7. The Fourier transform of the modulated total current in the 3-D simulation. This plot confirms the absence of nonaxisymmetric modes in the cavity.

4.0 CONCLUDING REMARKS AND FUTURE WORK

The radial acceletron, being a transit-time oscillator, latches onto a characteristic mode of the structure supporting it and produces a stable monochromatic radiation at a fixed frequency with little possibility of mode shifting or mode mixing. Furthermore, being an acceletron it allows the source to work at lower voltages ($\sim$250 kV) without forming a virtual cathode. It is called a *radial* acceletron in particular because of its radial mode of operation allows much lower impedances for the diode, leading to higher input/output powers at lower voltages ($\sim$10 ka of current for a 250 kV pulse). In addition, because there is no external magnetic field, the source is small, light, and portable. Also, because there are no foils necessary, potentially repetition rates are possible.

Numerical simulations have confirmed the viability of the concepts involved. The bunching and the gated emission features of the device are particularly encouraging. Switching to much higher frequencies with little or no drop in the power output is possible. The efficiency (rms), based on preliminary loading simulation results and bunching levels observed, could exceed 50 percent. The authors believe a 2 GW source in the x-band operating at 250 kV with a repetition rate of 1 kHz is possible.

Future work on the radial acceletron is basically optimization and load configuration. Once the loading is designed, a prototype for experimental testing can be built. Integration of the source into the pulser system and the antenna should not present any major problems. The Phillips Laboratory is planning an experimental test of the radial acceletron for early 1994.

REFERENCES

1. Marcuse, D., Principles of Quantum Electronics, pp. 125-144, Academic Press, New York, NY (1980).

2. Marcum, J., "Interchange of Energy Between an Electron Beam and an Oscillating Electric Field," *J. Appl. Phys.* 17 (4) (1946).

3. Godfrey, B. B., "Oscillatory Nonlinear Electron Flow in a Pierce Diode," *Phys. Fluids* 30, p. 1553 (1987).

4. Arman, M. J., D. J. Sullivan, B. B. Godfrey, R. E. Clark, J. E. Walsh, Analytical Study and Numerical Simulation of High Power Vircator and Transvertron Microwave Sources, MRC/ABQ-R-1029, Mission Research Corporation, Albuquerque, NM (1988).

5. Sullivan, D. J., J. E. Walsh, M. J. Arman, B. B. Godfrey, "Simulation of Transvertron High Power Microwave Sources," *SPIE's OE/LAS'*89 (1988).

Appendix

Sample MAGIC Input File

```
TITLE "Acceletron .25mv 25 ohm g=4.20cm l=8.0cm reflect" ;
TERMINATE WARNING ;
COMMENT "Low Impedence Radial acceletron " ;
SYSTEM CYLINDER-THETA ;
DIAGNOSE SPACING 1 0 0 ;
X1GRID FUNCTION  102 2 0.    100 .0040  .40 ;
X2GRID FUNCTION  50 2 0.18   42 .0060  .252
                 6 .0050  .030 ;
CONDUCTOR BASE      ALIGN 2, 7 30,7  30,2  36,2  36,7
                 44, 7 44,11 48,11 48,10 56,10 56,11
                 60,11 60,2 2,2  2,7 ;
CONDUCTOR CATHODE    ALIGN  48,11  56,11  ;
CONDUCTOR ANODE  ANTI-ALIGN  2,22  30,22  30,27  36,27  36,22
                 44,22  44,17, 60,17  60,50  102,50  ;
CONDUCTOR COAX    ANTI-ALIGN   81, 2  81,44  102,44  102,2  81,2 ;
FIELDS TM CENTERED 20001 1.E-11 ;
TIMER LAST PERIODIC 70000 999999 70000 ;
RECORD LAST "RSTART" 2 ;
COURANT SEARCH ;
FIELD-EMISSION INJECTION ELECTRON 1 1 STEPPED RANDOM 4.E-5
          UNIFORM MOMENTUM 1.E6 1. 5.E5 0. 0. 0. ;
EMIT INJECTION CATHODE ;
KINEMATICS ELECTRON 1 YES NO NO EM  1 1 ;
CURRENTS LCC NO NO  0 1. ;
FORCES  .5  1.  1. ;
FUNCTION INLEFT   DATA  3   0.      0.
                 10.E-9    2.5E5
                 100.E-8   2.5E5 ;
FUNCTION "FOR(R)=1./R" ;
VOLTAGE FIELDS TM INLEFT  FOR 1.  0.  1.     ALIGN  2   7  2 22 ;
LOOKBACK FIELDS TM 1. 1. ANTI-ALIGN  102  50   102  44 ;
```

```
SYMMETRY MIRROR ALIGN 60 2  60 2 ;
DISPLAY INTEGER 2 102 2 50 ;
TIMER PRPL PERIODIC  1 100000 5000 ;
PERSPECTIVE PRPL FIELD E1 2, 102 2,50 1 1 ;
PERSPECTIVE PRPL FIELD E2 2, 102 2,50 1 1 ;
PERSPECTIVE PRPL FIELD B3 2, 102 2,50 1 1 ;
CONTOUR PRPL FIELD E1 2, 102 2,50 ;
CONTOUR PRPL FIELD E2 2, 102 2,50 ;
VECTOR PRPL FIELD B3 B3 AXIS X 0. .40 SCALE LOG 2 ;
VECTOR PRPL FIELD E1 E2 AXIS X 0. .40 SCALE LOG 2 ;
VECTOR PRPL FIELD J1 J2  AXIS X 0. .40 ;
RANGE PRPL 1 FIELD E2 2 13  102 13 ;
RANGE PRPL 1 FIELD E1 2 13  102 13 ;
RANGE PRPL 1 FIELD E2 52 2  52 50 ;
TIMER SCAT PERIODIC  5000 100000 5000 ;
TAGGING 1. ;
TRAJECTORY 5000 SCAT 1 ELECTRON  0. .40 .18 .462 ;
PHASESPACE SCAT AXES X1 X2
          AXIS X 0.  .40
          AXIS Y 0.18 .462
          SELECT TAG ;
C **** PHASESPACE SCAT AXES X1 P1
C ****        AXIS X 0.  .40
C ****        AXIS Y -1.E8 1.E8
C ****        SELECT TAG ;
PHASESPACE SCAT AXES X2 P2
          AXIS X 0.18  .462
          AXIS Y -5.E8 5.E8
          SELECT TAG ;
TIMER STAT PERIODIC  1 100000 100 ;
STATISTICS STAT ;
TIMER ENG PERIODIC  1 100000  10 ;
ENERGY ENG 2 102 2 50 ;
OBSERVE WINDOW FREQUENCY 1.E9 20.E9 ;
OBSERVE FIELD E2   52 12  52 12 INTERVAL 2 FFT 5 ;
OBSERVE FIELD E2   52 14  52 11 INTERVAL 2 FFT 5 ;
```

```
OBSERVE FIELD E2    52 18   52 11  INTERVAL  2 FFT 5 ;
OBSERVE FIELD E1    44 14   60 14  INTERVAL  2 FFT 5 ;
OBSERVE FIELD J2   102 12    2 12  INTERVAL  2 FFT 5 ;
OBSERVE FIELD J2   102 15    2 15  INTERVAL  2 FFT 5 ;
OBSERVE FIELD B3     3 21    3 21  INTERVAL  2 FFT 5 ;
OBSERVE FIELD E2     3  7    3 50  INTERVAL  2 FFT 5 ;
OBSERVE FIELD E2   101  2  101 50  INTERVAL  2 FFT 5 ;
OBSERVE WINDOW FREQUENCY  1.E8 40.E9;
OBSERVE ENERGY VOLTAGE   1  0  INTERVAL 2 FFT 5 ;
OBSERVE ENERGY LOOKBACK   1  0  INTERVAL 2 FFT 5 ;
START ;
STOP ;
```